

# Accessory pathway localization with probabilistic density maps generated by a mobile application: Validation of a full preexcitation net-vector method

Marek Jastrzebski<sup>1</sup>, Kamil Fijorek<sup>2</sup>, Piotr Futyma<sup>3</sup>, Michal Orczykowski<sup>4</sup>, Maciej Pitak<sup>5</sup>, Łukasz Zarębski<sup>3</sup>, Piotr Sajdak<sup>3</sup>, Sebastian Góreczny<sup>5</sup>, Łukasz Szumowski<sup>4</sup>, Rajzer Marek<sup>1</sup>, and Pawel Moskal<sup>6</sup>

<sup>1</sup>Uniwersytet Jagiellonski w Krakowie I Klinika Kardiologii i Nadciśnienia Tętniczego

<sup>2</sup>Uniwersytet Ekonomiczny w Krakowie

<sup>3</sup>Uniwersytet Rzeszowski

<sup>4</sup>National Institute of Cardiology

<sup>5</sup>Uniwersytet Jagiellonski w Krakowie Collegium Medicum

<sup>6</sup>Szpital Uniwersytecki w Krakowie

April 12, 2024

## Abstract

**Introduction.** Precise electrocardiographic localization of accessory pathways (AP) can be challenging. Seminal AP localization studies were limited by complexity of algorithms and sample size. We aimed to create a non-algorithmic method for AP localization based on color-coded maps of AP distribution generated by a web-based application. **Methods.** APs were categorized into 19 regions/types based on invasive electrophysiologic mapping. Preexcited QRS complexes were categorized into 6 types based on polarity and notch/slur. For each QRS type in each lead the distribution of APs was visualized on a gradient map. The principle of common set was used to combine the single lead maps to create the distribution map for AP with any combination of QRS types in several leads. For the validation phase, a separate cohort of APs was obtained. **Results.** A total of 804 patients with overt APs were studied. The application used the exploratory dataset of 552 consecutive APs and the corresponding QRS complexes to generate AP localization maps for any possible combination of QRS types in 12 leads. Optimized approach (on average 3 steps) for evaluation of preexcited ECG was developed. The area of maximum probability of AP localization was pinpointed by providing the QRS type for the subsequent leads. The exploratory dataset was validated with the separate cohort of APs ( $n = 260$ );  $p = 0.23$  for difference in AP distribution. **Conclusions.** In the largest dataset of APs to-date, a novel probabilistic and semi-automatic approach to electrocardiographic localization of APs was highly predictive for anatomic localization.

## Introduction.

Catheter ablation is an important curative therapy for arrhythmias and sudden cardiac death caused by accessory pathways (AP). (1-3) An important part of catheter ablation is precise electrocardiographic localization of AP localization along the mitral and tricuspid annuli. AP capable of orthodromic conduction influences QRS morphology by preexciting the adjacent ventricular myocardium. The preexcited QRS configuration depends on the localization of the AP and the degree of preexcitation. Those observations form the foundation of all ECG based methods for APs localization.

Precise electrocardiographical localization of AP remains an elusive goal. Despite various complex algorithms that were developed over the last three decades, accuracy is suboptimal - as demonstrated by several

independent validation studies. (4-9) Moreover, those detailed algorithms are difficult to remember and follow which further limits their practical application. The inherent limitation of all AP algorithms stems from the fact that the AP regions used by the algorithms are categorical, rather than along a spectrum. The same applies to ECG features such as QRS polarity or delta wave polarity, which do not follow binary categorization. Furthermore, uniform 12 ECG lead placement cannot compensate for the variability in heart position within the chest and oblique APs. Therefore, it is unrealistic to expect that some combination of QRS morphologies in 12 ECG leads will precisely identify a particular AP region in a 0 vs. 1 fashion.

We hypothesized that 12-lead ECG QRS morphology patterns point to a region of possible AP locations, albeit with identification of the anatomic sites with highest probability.

## Aims

To develop and validate a novel and non-algorithmic and semi-automatic method for AP localization based on colour-coded gradient maps that indicate the probability of AP localization.

To propose an optimized stepwise approach to preexcited ECG by a net-vector analysis - supported by the web-based mobile application.

## Methods

The study was conducted according to the Helsinki declaration and was approved by local bioethical committee.

### *Population*

The purpose of the exploratory phase was to build a web-based application capable of generating representative density maps of AP localization. Consecutive patients who underwent AP ablation in two centres over a 17-year period (2001-2018) were retrospectively screened. Patients with concealed preexcitation, poor ECG quality, uncertain ablation site or unsuccessful ablation were excluded.

### *Categorization of accessory pathway regions/types*

The AP categorization is illustrated by the diagram on **Figure 1** and explained in detail below. For anatomic localization of the ablation site, fluoroscopic imaging or electroanatomic 3D maps were used in various projections, especially the left anterior oblique projection of 35 degree (LAO).

- Parahisian (PHIS) localization was diagnosed when a His bundle potential was recorded at the site of successful ablation.
- Right midseptal (RMS) region was defined as below the PHIS region and above the roof of the coronary sinus ostium.
- Right posteroseptal (RPS) region was defined as below the roof of the coronary sinus ostium, including the periostial region (but less than 1 cm inside the coronary sinus) and extending to 5.00 o'clock on the tricuspid annulus in LAO.
- Right posterior (RP) region was defined as between 5.00 and 7.00 o'clock on the tricuspid annulus in LAO.
- Right posterolateral (RPL) region was defined as between 7.00 and 8.00 o'clock on the tricuspid annulus in LAO.
- Right lateral region (RL) region was defined as between 8.00 and 10.00 o'clock on the tricuspid annulus in LAO.
- Right anterolateral (RAL) region was defined as between 10.00 and 11.00 o'clock on the tricuspid annulus in LAO.
- Right anterior (RA) region was defined as between 11.00 and 12.30 o'clock on the tricuspid annulus in LAO.
- Right anteroseptal (RAS) region was defined as between 12.30 o'clock on the tricuspid annulus in LAO and the PHIS region.

- Epicardial (EPI) AP was diagnosed when the successful ablation had to be performed within the coronary sinus (> 1 cm from the ostium) including cardiac veins and coronary sinus diverticula.
- Atriofascicular (MAHAIM) AP was diagnosed per the recognized electrophysiological criteria for such AP, regardless of the actual position of successful ablation site on the tricuspid annulus.
- Fasciculoventricular (FASC-VENT) AP was diagnosed with HV < 35 ms and fixed preexcitation during incremental pacing, adenosine administration and/or extrastimulus testing.
- Left midseptal (LMS) AP was diagnosed when successful ablation was on the mitral annulus just below the His bundle potential region – corresponding in LAO to the right midseptal region.
- Left posteroseptal (LPS) region was defined as just below the aorta on the mitral annulus between 7.00 – 8.00 o'clock in LAO.
- Left posterior (LP) region was defined as between 5.00 – 7.00 o'clock on the mitral annulus in LAO.
- Left posterolateral (LPL) region was defined as between 4.00 – 5.00 o'clock on the mitral annulus in LAO.
- Left lateral (LL) region was defined as between 2.00 – 4.00 o'clock on the mitral annulus in LAO.
- Left anterolateral (LAL) region was defined as between 12.30 – 2.00 o'clock on the mitral annulus in LAO.
- Left anterior (LA) region (including aortomitral continuity), was defined as between 11.00-12.30 o'clock on the mitral annulus in LAO.

### *ECG assessment*

For each patient, ECG with baseline preexcitation and/or ECG with full preexcitation were analysed (per availability). Full preexcitation ECG pattern was obtained during electrophysiological study via incremental atrial pacing, programmed atrial pacing or adenosine administration. QRS polarity/type was coded as one of the six following categories: completely positive (monophasic R) without notches, completely positive (R) with notches (notch/plateau at the top of monophasic R wave), predominantly positive (Rs, Rsr', qR etc.), equiphasic (RS, QRS, RSR', etc.), predominantly negative (Qr, rS, rSr', etc.) or completely negative (QS) - depending on the dominant polarity. Examples of QRS categories are presented in **Figure 2** and inside the application next to each question. Most representative full preexcitation patterns for the 19 regions are illustrated in **Figure 3** and Supplementary **Figures 1-2**.

### *Mobile web-based application (WPW24.com)*

Each AP region, and all QRS types in all 12 leads, separately for the full and baseline preexcitation patterns, were coded and introduced into the application database to enable automatic cross-correlation between AP localization and QRS morphology. A web-based application (WPW24.com), optimized for mobile devices was developed. The WPW24.com is a client side only progressive web app implemented with React and TypeScript. The application enabled to graphically show changing distribution of APs with regard to the introduced by the user, at each step, the QRS type in a particular ECG lead. Providing the QRS type for the subsequent ECG leads, pinpoints, in a stepwise manner, the area of maximum probability of AP localization (**Figures 4 - 6** and **Supplementary Video 1**). User can choose his/her own criteria/steps; there is no need to adhere to any steps or order of assessment of ECG leads. Both baseline and fully preexcited ECG can be used for map generation - per user preference. Each question regarding morphology is provided with a support – graphical illustration of several QRS types that are compatible with that QRS morphology category.

### *Proposed steps of ECG assessment to localize AP*

Optimized steps for ECG analysis were added to the WPW24.com app to increase its functionality. These steps were developed on the basis of the classic rules of ECG interpretation and the personal experience of over 1000 APs ablated by the first author. Most of these criteria, in various modifications, can be found in the literature, (10-17) the only authorial criterion is QRS notch/slur/plateau (**Figure 2**) to differentiate right free wall pathways from septal pathways. The steps for ECG analysis were optimized by post-hoc assessment - if a step did not result in an expected differentiating change of AP distribution pattern – it

was abandoned and other were explored. Following rules were tested to build the pathways for analysis of preexcited ECG:

1. Positive or equiphasic V1 indicates left free wall and left septal AP; conversely, negative V1 indicates right free wall and right septal AP
2. Precordial transition to positive/equiphasic QRS at V2 – V4 indicates right septal AP; while precordial transition > V4 suggest right free wall or Mahaim AP
3. Negative II, III, aVF indicate posterior AP, positive II, III, AVF indicate anterior AP, while mixed polarity in these leads suggest sites in-between (i.e. lateral free-wall or midseptal). In such scenario, right free wall pathways are favored by the presence of a notch/slur/plateau in leads I, aVL, aVF or V6.
4. Completely positive lead I indicates right or septal AP. Contrarywise, the more negative the QRS in lead I (the deeper the S wave) the more to the left is the AP, with completely negative complex (QS morphology) indicating the most left sided region – i.e. left lateral location.

### *Statistics*

Continuous variables are presented as means and standard deviations. Categorical variables are presented as percentages. Comparison of APs distribution patterns between groups were made using the Ch2 and Wilcoxon tests. Weighted Kappa-statistic was used to assess the inter-observer agreement. Statistical analyses were performed using STATA 18 (StataCorp, Texas, USA). P-values < 0.05 were considered statistically significant.

### *Validation*

Since the outcome of the WPW24.com based ECG analysis does not point to a single AP location but to a spectrum of anatomic locations with a gradient of probability – validation of the method in a traditional manner (i.e., the predicted site vs. the site of successful ablation) was not feasible. Even apparently very odd AP locations (for a particular QRS pattern) suggested by the WPW24.com might be validated as correct when a sizable number of APs, that included such rare variants, is analysed. Therefore, to validate WPW24.com, we examined whether the distribution of APs used by the application to generate the maps is representative. Validation of distribution patterns was performed only for the full preexcitation as inherently more precise. For this, comparison of AP distribution in the exploratory cohort that was used by the application with the AP distribution in two external cohorts was made. The first dataset used for validation was obtained from new patients studied in years 2018-2023 in four centres. The second dataset for validation of AP distribution was obtained from the seven published studies that proposed new AP localization algorithms. The validation phase was commenced once the work on the web-based application, and the exploratory cohort, were completed.

## **Results**

A total of 804 consecutive patients (age:  $30.9 \pm 18.6$  years; male: 58.6%) with overt preexcitation were studied. These patients provided 547 with baseline preexcitation and 769 ECGs with full preexcitation.

### *Exploratory and validation phases*

The first 546 consecutive patients provided dataset of AP localization and QRS morphology types in 12 leads including 509 ECGs with full preexcitation and 547 ECGs with baseline preexcitation that were furnished to the WPW24.com database. Distribution of all APs in that cohort is presented in **Figure 1** and **Table 1**. Illustrative examples of how QRS polarity in a single ECG lead impacts distribution of APs along mitral and tricuspid annuli is presented in **Figure 5** and **6**. Depending on the AP type/localization there were 2 to 5 optimized steps for ECG analysis. To reach the final diagnosis/distribution map a mean  $3.0 \pm$  steps per ECG were needed.

For validation, the dataset of 260 ECGs were used, 49% of these ECGs were obtained prospectively, after the exploratory phase. The remaining 51% were obtained retrospectively albeit from a new centre that did

not participate in the exploratory phase. Distribution of all APs in the exploratory and validation phases is presented in **Figure 1** and **Table 1** – no differences in the distribution of APs between the exploratory and validation datasets were found ( $p = 0.263$ ).

To compare the exploratory cohort with the data from the literature a simplified categorization of AP regions had to be applied since the categorization and regions in every study are different, sometimes poorly defined and often with overlap of different regions among studies, making direct detailed comparison impossible (**Supplementary Table 1**). However, when all AP were grouped into four major categories (right free wall, left free wall, right posteroseptal and other septal) no difference in the distribution of AP among the exploratory cohort and the pooled cohort from the seven published studies ( $n = 1252$ ), was present,  $p = 0.24$ .

#### *Baseline and maximal preexcitation*

Both baseline and full preexcitation based ECG analysis were implemented in WPW24.com to enhance its functionality. However, the baseline preexcitation maps showed wider spread of regions than full preexcitation maps indicating lower value of fused QRS vectors for AP localization. For formal comparison of baseline and full preexcitation AP distribution maps three differentiating QRS polarities were chosen: lead V1 negative/predominantly negative, lead I positive/predominantly positive, lead III positive/predominantly positive. For each of these polarities APs distribution were compared between baseline and full preexcitation confirming differences in distribution ( $p < 0.05$ ); for visual assessment see **Supplementary Figure 3**.

#### *Miscellaneous*

A total of 50 consecutive ECGs were analysed by a second observer. Interobserver agreement of QRS polarity assessment was very high (agreement 94.27%, kappa 0.8931, and standard error 0.033,  $p < 0.0001$ ).

## **Discussion**

The major results of the study were as below:

1. The method for AP localization with AP distribution gradient maps – separate for any specified 12-lead preexcited QRS pattern was developed and supported by a dedicated mobile application.
2. The hypothesis that a particular 12-lead QRS morphology pattern will point to a wider area of possible AP locations, rather than to a single location was verified with the observed AP distribution patterns in a large cohort.
3. Optimized stepwise approach for analysis of preexcited ECG was developed.

#### *Comparison with the algorithmic methods for AP localization*

Majority of AP localization algorithms were based on a limited number of cases, often partially pre-selected. For example, the sample size was 120, 157, 140, 135, 93 and 148 in Ferrari et al., Boersma et al, D'Avila et al., Arruda et al., Fitzpatrick et al., and Millstein et al. algorithms, respectively. (10-13;15;16) Small sample size can create an illusion that a particular QRS pattern is 100% specific for some location – as it is not seen at other AP locations. However, a bigger sample might show that other cases with the same ECG pattern had successful ablation at other locations as well. The current study, based on the largest cohort of overt AP ever studied, fully supports the concept that preexcited ECG pattern does not point to a particular location but rather reflects a wider area, albeit with the site of maximum AP frequency surrounded by a probability gradient. Representative illustration of this phenomenon can be found on **Supplementary Figure 4**, which presents outcomes of analysis of the same ECG with the D'Avila algorithm and with WPW24.com app.

Algorithms are trying to create an ideal match between AP location and QRS pattern. Imperfections of that match are covered by algorithm's sensitivity and specificity. Several independent validation studies showed that sensitivity/specificity/accuracy of algorithmic methods are lower than initially reported. These studies are in agreement with the current results, because low accuracy of an algorithm indicates that the APs were not limited to the single predicted locations but probably there was a wider spread of APs. Consequently, algorithmic methods are a somewhat misleading by creating an illusion of single location even when their

sensitivity, specificity and accuracy are low - indicating contrariwise. In contrast, WPW24.com, instead of pretending precision and pointing to one location is showing where the accessory pathways were actually ablated in all studied cases with the QRS pattern that is similar or identical to the one with which the current patient had presented.

Almost all algorithms are based on the analysis of baseline preexcited ECG, occasionally, on ‘most preexcited’ baseline ECG – that is on a QRS morphology that results from fusion between native conduction and AP conduction. That might be another reason for the divergence between the original studies and the independent validation studies – as the degree of preexcitation for the same localization varies and it is impossible to determine how much preexcited ECGs were used in the original study. Full preexcitation pattern maximizes the localizing information contained in the preexcited QRS polarity because the confounding impact of conduction via His-Purkinje system on QRS is nearly eliminated. Moreover, full preexcitation standardizes the ECG patterns for comparison between studies. It was shown in our previous work that using fully preexcited ECG increases accuracy of AP localization, even for algorithms that were designed for analysis of baseline preexcitation. (6)

### *Clinical translation*

Operators are nowadays more familiar with 3D colour-coded gradient maps than with preexcitation patterns in ECG. A tool that supports AP localization in a familiar fashion, with color-coded gradient map that covers the mitral and tricuspid rings, may be a more descriptive and predictive method to enhance utility of standard 12-lead ECG for the assessment and treatment of WPW cases. Moreover, the WPW24.com app has a substantial educational potential by illustrating the relationship between changing morphology of QRS and the related changes in AP distribution along the tricuspid and mitral annuli (**Figures 6 and Supplementary Figure 1**).

Algorithms are often complex, introduce subjectivity with binary categorizations, and are difficult to memorize. The polarity of the initial 20 ms of the delta wave, used in several algorithms, is often difficult to discern and has significant inter-observer variability. In our experience, algorithms are rarely followed in real life practice, but physicians rather use simple set of rules, similar to these on which the current method was based. The WPW24.com addresses these limitations by being readily available to any smartphone or tablet user without the need to memorize anything. And, by being based on the QRS polarity (net vector) - a feature so easy to ascertain, especially with the provided inside app examples of different QRS configurations that are compatible with a particular category (**Figure 2**), makes the preexcited ECG analysis straightforward.

Use of an algorithm, that indicates one particular AP location, can fix the operator on undue pursuit of ablation in that region even when multiple energy applications were not successful. A gradient map by being more honest with regard to the possible AP locations, while directing to the most probable area as well, gives also clues what other locations should be explored in the next steps. For example, even quite typical ECG pattern for RPS site (QRS transition to positive at V2, negative II) is sometimes seen with AP at RMS, RP, LMS, LPS, and EPI locations.

WPW24.com can be seen as a tool for memory enhancement and sharing of experience. A small-volume AP ablationist might have never experienced or likely does remember a patient ablated several years ago, that had a rare preexcited ECG pattern that was identical to the ECG of the patient currently on the table. Yet that pattern could be an excellent clue to the localization of the AP that is undergoing ablation. Illustration of such scenario that occurred during the current study is presented in **Figure 1** and **Supplementary Video 1**. In the future, WPW24.com database can be expanded by adding datasets of consecutive APs from other centers, getting as close as possible to making precise diagnosis of AP type/location via full 12-lead QRS pattern recognition.

### *Limitations*

Given the non-categorical and non-algorithmic nature of our probability maps - direct comparison with

other methods was not possible. Moreover, it was not possible to quantify accuracy and traditional test characteristics like specificity and sensitivity.

### Conclusions

A novel method for electrocardiographic localization of APs, based on a probabilistic approach and semi-automatic analysis of QRS patterns from the largest to-date cohort of overt AP is predictive, accurate, with high reproducibility. Anatomic localization that is based on probabilistic gradient maps of AP distribution may be more accurate than historical categorizations.

### Funding

The study was supported by the PTK SENIT grant number K/DAR/000001

### Acknowledgments

We gratefully acknowledge the assistance of Roderick Tung in reviving and preparing the final manuscript.

### Figures and legends

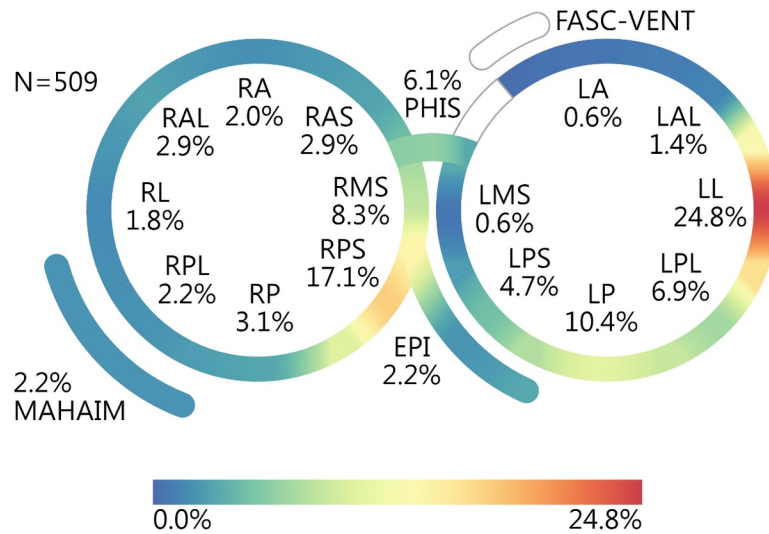


**Figure 1.** Categorization of accessory pathway (AP) regions/types. This is the baseline probability map of AP localization that is the starting point of ECG interpretation - before any QRS morphology data is considered by the WPW24.com application. The percentages correspond to the distribution of all AP in the full preexcitation cohort - hence the fasciculo-ventricular pathways, not capable to fully preexcite the ventricles, are not counted here. For explanation of the abbreviations and the definitions of AP types/regions see text.

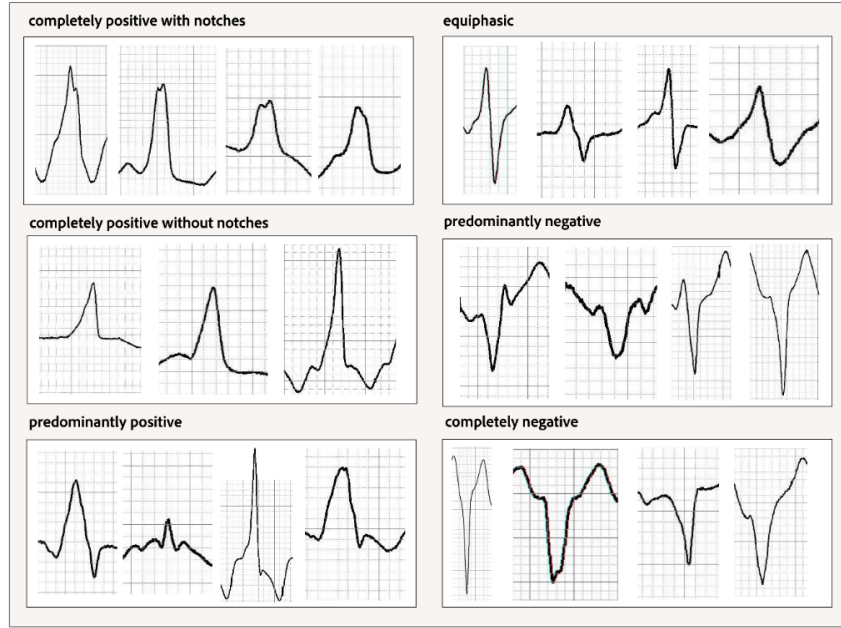


**Figure 2** . Six categories of fully preexcited QRS morphology. Regardless of the number of deflections in QRS, the overall polarity is defined by the dominant deflection, e.g. rSr is a predominantly negative QRS. Equiphasic QRS is diagnosed when none of the deflections is  $> 2$  mm than the other.

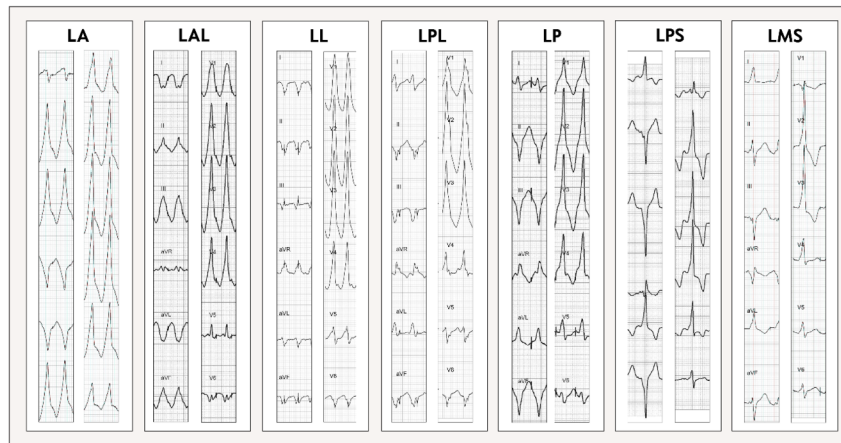


**Figure 3** . Representative examples of fully preexcited QRS complexes of accessory pathways ablated from the left side. Most lateral sites (LA, LAL, LL, LPL) are characterized by QS/rS in lead I and high amplitude V1, Contrariwise, septal/paraseptal sites (LP, LPS, LMS) have R/RS wave in lead I and often small amplitude/multiphasic QRS in V1. Lead aVF differentiates between superior (R) and inferior locations (QS/rS). Representative examples of fully preexcited QRS complexes of accessory pathways ablated from the right side are in Supplementary Figures 1 and 2. For abbreviations see text.

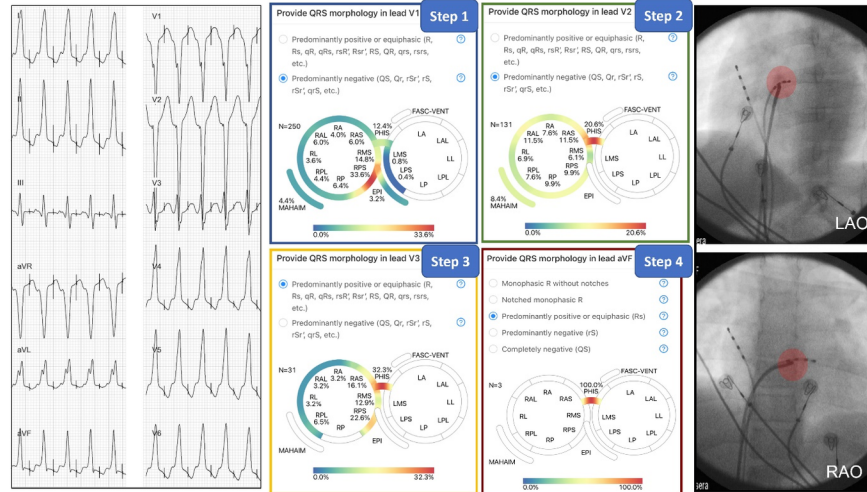


**Figure 4.** Illustration of the ECG analysis via WPW24.com application at the beginning of the ablation procedure. Left panel: the fully preexcited QRS is obtained with fast atrial pacing. At steps 1-4 the information regarding QRS morphology is introduced into the application. *Step 1* : predominantly negative V1 nearly eliminates the left sided access accessory pathways (AP), only small admixture of left septal APs remains, the point of maximum is now at the most common right-sided region i.e. right posteroseptal (RPS). *Step 2* : predominantly negative QRS in V2 now eliminates the possibility of left sided APs and makes RPS AP relatively unlikely, shifting the point of maximum probability to the parahisian region (PHIS) and adjoining right anteroseptal (RAS) region, but many other right-sided locations are also possible. *Step 3* : equiphasic QRS in V3 lowers the chances of a right free wall AP and shifts the focus to septal pathways as 50% of possible APs are now at the PHIS or RAS regions. *Step 4* : predominantly positive aVF, intuitively, should eliminate posterior pathways (RPS, RMS, RP i RPL), but it does more than that: it identifies a rare QRS pattern that was seen only 3 times per 509 APs and in all those three cases (from the exploratory cohort) the successful ablation was in the PHIS region. In this fourth case analysed, (from the validation cohort) the successful ablation (left panels) was also in the PHIS region.

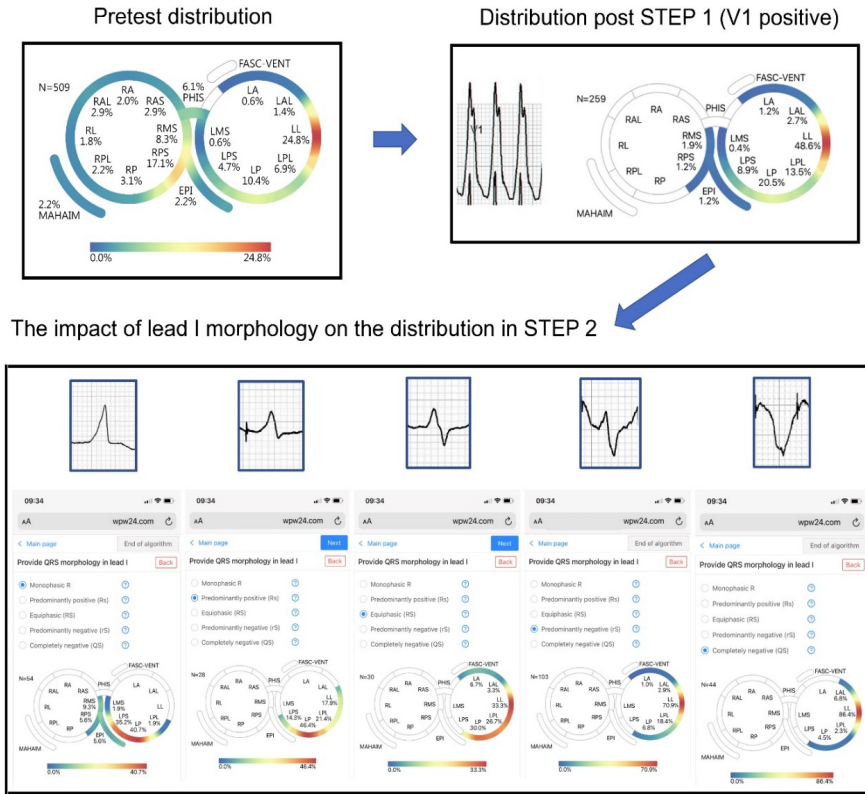


**Figure 5.** The impact of fully preexcited QRS morphology in lead I fully on the distribution of accessory pathways (APs). Positive V1 at the *STEP 1* changes the pretest AP distribution by eliminating almost all right-sided APs, only a small admixture of right-sided septal APs remains. At the *STEP 2* : QRS morphology in lead I has to be provided. With increasing negativity of the QRS in lead I, the maximum probability site shift progressively to the left. A QS complex in lead I identifies left lateral (LL) AP, with 86.4% of all such APs ablated at that region, while R complex in lead I eliminates the possibility of LL AP and shifts point of maximum probability to the left posterior location (LP, 40.7%); common alternative sites are the adjacent left posteroseptal (LPS, 35.2%) and septal/epicardial (23%). With Rs or RS complex one more step is necessary to reach the final diagnosis, while with R, rS or QS complex the second step is the final step.

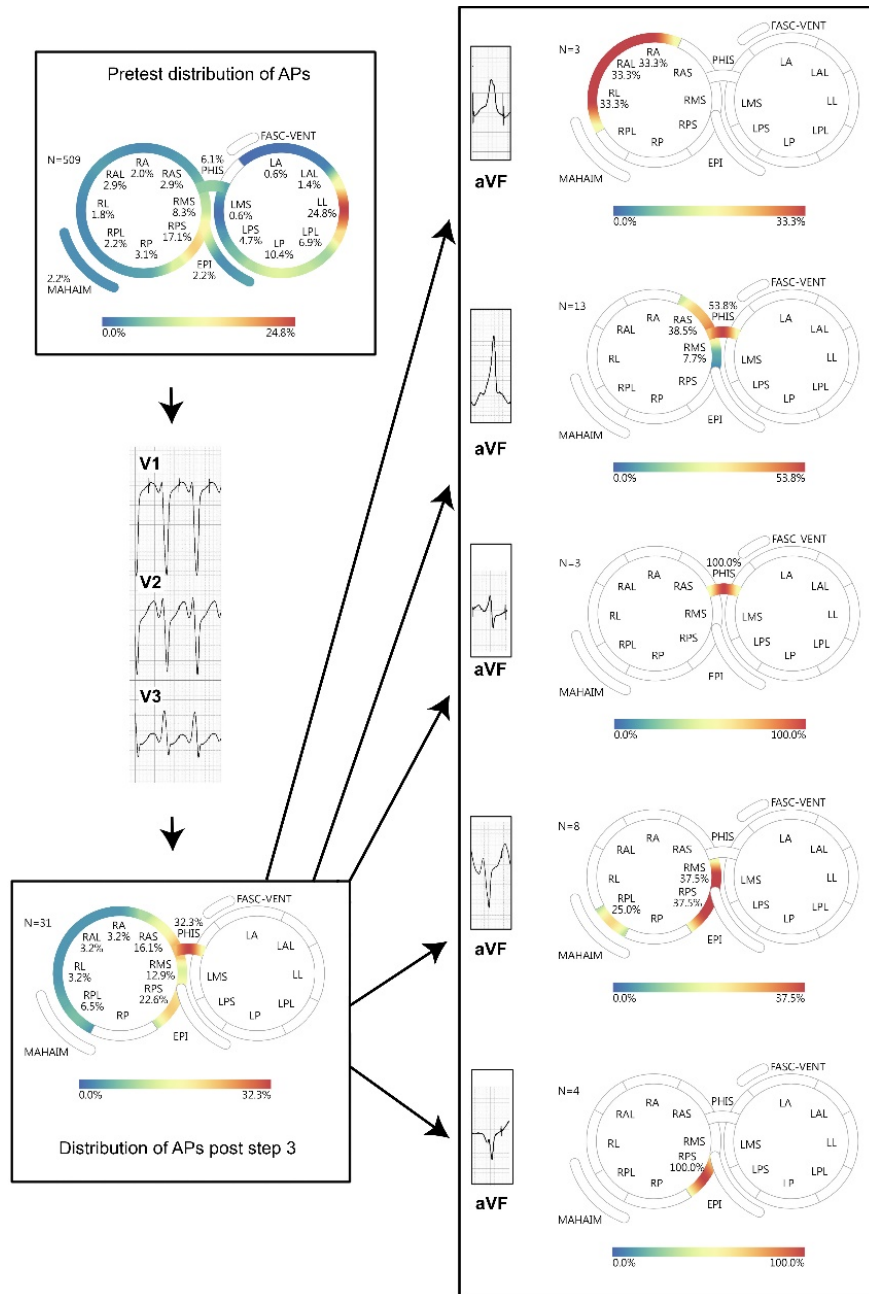


**Figure 6.** Impact of fully preexcited QRS morphology in lead aVF on the distribution of accessory pathways (APs) in patients with transition from negative QRS to positive QRS at V3. The right panel illustrates how, first with the disappearance of notch/slur the localization of APs shifts from the free wall to the septum, and then, with increasing negativity in lead aVF the point of maximum density shifts progressively more inferiorly on the septum (maps from the top to the bottom in the right panel).

**Table 1 .** Distribution of overt accessory pathways (AP) among regions/types in the current study and the literature.

AP region	Current study	Exploratory Validation		Milstein n = 148	Ferrari n = 120	Arruda n = 256	Pambrun n = 339	D'Avila n = 139	Fitzpatrick n = 93
	all n = 808	cohort n = 552	cohort n = 256						
Parahisian	5.2 (42)	5.8 (32)	3.9 (10)	-	-	-	7.4 (25)	-	-
Right midseptal	7.8 (63)	7.8 (43)	7.8 (20)	31.8 (47)	15 (18)	3.5 (9)		7.2 (10)	7.5 (7)
Right posteroseptal	18.9 (153)	17.4 (96)	22.3 (57)		13 (16)	17.6 (45)	17.7 (60)	21.6 (30)	18.3 (17)
Right posterior	2.5 (20)	3.1 (17)	1.2 (3)	3.4 (5)	1.5 (2)	2.3 (6)	6.8 (23)		9.7 (9)
Right posterolateral	2.1 (17)	2.4 (13)	1.6 (4)		-	3.1 (8)	-	7.9 (11)	
Right lateral	2.3 (19)	1.8 (10)	3.5 (9)		5 (6)	7.0 (18)	2.4 (8)		
Right anterolateral	2.6 (21)	2.7 (15)	2.3 (6)		4 (5)	2.7 (7)	-	-	12.9 (12)
Right anterior	2.1 (17)	2.0 (11)	2.3 (6)		3 (4)	7.0 (18)	5.0 (17)	-	
Right anteroseptal	2.2 (18)	2.7 (15)	1.2 (3)	13.5 (20)	12 (15)	6.2 (16)		18.0 (25)	11.8 (11)
Epicardial	2.6 (21)	2.2 (12)	3.5 (9)	-	-	8.2 (21)	2.1 (8)		-
Atriofascicular	2.0 (16)	2.2 (12)	1.6 (4)	-	-	-	-	-	-
Fasciculoventricular	2.0 (11)	2.0 (11)	-	-	-	-	-	-	-
Left midseptal	0.7 (6)	0.5 (3)	1.2 (3)	-	-	-	-	-	-
Left posteroseptal	5.3 (43)	4.5 (25)	7.0 (18)	51.4 (76)	11 (13)	4.2 (11)	12.4 (42)	7.9 (11)	5.4 (5)
Left posterior	8.8 (71)	10.0 (55)	6.2 (16)		3 (3)	2.3 (6)		5.0 (7)	14.0 (13)
Left posterolateral	8.0 (65)	6.5 (36)	11.3 (29)		6 (7)	5.9 (15)	14.1 (48)		
Left lateral	22.9 (185)	24.6 (136)	19.1 (49)		24 (29)	18.7 (48)	31.9 (108)	32.4 (45)	20.4 (19)
Left anterolateral	1.9 (15)	1.3 (7)	3.1 (8)		2 (2)	10.9 (28)			
Left anterior	0.6 (5)	0.5 (3)	0.8 (2)		-	-	-	-	-

## References

1. Jastrzebski M, Moskal P, Pitak M, Fijorek K, Rudzinski A, Czarnecka D. Contemporary outcomes of catheter ablation of accessory pathways: complications and learning curve. *Kardiol Pol* 2017;75:804-810.
2. Moskal P, Jastrzebski M, Pitak M, Fijorek K, Werynski P, Czarnecka D. Malignant ventricular arrhythmias and other complications of untreated accessory pathways: an analysis of prevalence and risk factors in over 600 ablation cases. *Kardiol Pol* 2020;78:203-208.
3. Orczykowski M, Walczak F, Derejko P, Bodalski R, Urbanek P, Zakrzewska-Koperska J et al. Ventricular

fibrillation risk factors in over one thousand patients with accessory pathways. *Int J Cardiol* 2013;167:525-530.

4. Basiouny T, De CC, Fareh S, Kirkorian G, Messier M, Sadoul N et al. Accuracy and limitations of published algorithms using the twelve-lead electrocardiogram to localize overt atrioventricular accessory pathways. *J Cardiovasc Electrophysiol* 1999;10:1340-1349.
5. Katsouras CS, Greakas GF, Goudevenos JA, Michalis LK, Kolettis T, Economides C et al. Localization of accessory pathways by the electrocardiogram: which is the degree of accordance of three algorithms in use? *Pacing Clin Electrophysiol* 2004;27:189-193.
6. Moskal P, Bednarski A, Kielbasa G, Czarnecka D, Jastrzebski M. Increased preexcitation on electrocardiography improves accuracy of algorithms for accessory pathway localization in Wolff-Parkinson-White syndrome. *Kardiol Pol* 2020;78:567-573.
7. Wren C, Vogel M, Lord S, Abrams D, Bourke J, Rees P et al. Accuracy of algorithms to predict accessory pathway location in children with Wolff-Parkinson-White syndrome. *Heart* 2012;98:202-206.
8. Maden O, Balci KG, Selcuk MT, Balci MM, Acar B, Unal S et al. Comparison of the accuracy of three algorithms in predicting accessory pathways among adult Wolff-Parkinson-White syndrome patients. *J Interv Card Electrophysiol* 2015;44:213-219.
9. Teixeira CM, Pereira TA, Lebreiro AM, Carvalho SA. Accuracy of the Electrocardiogram in Localizing the Accessory Pathway in Patients with Wolff-Parkinson-White Pattern. *Arq Bras Cardiol* 2016;107:331-338.
10. Arruda MS, McClelland JH, Wang X, Beckman KJ, Widman LE, Gonzalez MD et al. Development and validation of an ECG algorithm for identifying accessory pathway ablation site in Wolff-Parkinson-White syndrome. *J Cardiovasc Electrophysiol* 1998;9:2-12.
11. d'Avila A, Brugada J, Skeberis V, Andries E, Sosa E, Brugada P. A fast and reliable algorithm to localize accessory pathways based on the polarity of the QRS complex on the surface ECG during sinus rhythm. *Pacing Clin Electrophysiol* 1995;18:1615-1627.
12. Milstein S, Sharma AD, Guiraudon GM, Klein GJ. An algorithm for the electrocardiographic localization of accessory pathways in the Wolff-Parkinson-White syndrome. *Pacing Clin Electrophysiol* 1987;10:555-563.
13. Ferrari P, Malanchini G, Racheli M, Ferrari G, Leidi C, Cerea P et al. Can we improve the accuracy of electrocardiographic algorithms for accessory pathway location in children? *Kardiol Pol* 2022;80:33-40.
14. Pambrun T, El BR, Combes N, Combes S, Sousa P, Le BM et al. Maximal Pre-Excitation Based Algorithm for Localization of Manifest Accessory Pathways in Adults. *JACC Clin Electrophysiol* 2018;4:1052-1061.
15. Fitzpatrick AP, Gonzales RP, Lesh MD, Modin GW, Lee RJ, Scheinman MM. New algorithm for the localization of accessory atrioventricular connections using a baseline electrocardiogram. *J Am Coll Cardiol* 1994;23:107-116.
16. Boersma L, Garcia-Moran E, Mont L, Brugada J. Accessory pathway localization by QRS polarity in children with Wolff-Parkinson-White syndrome. *J Cardiovasc Electrophysiol* 2002;13:1222-1226.
17. Reddy GV, Schamroth L. The localization of bypass tracts in the Wolff-Parkinson-White syndrome from the surface electrocardiogram. *Am Heart J* 1987;113:984-993.